Prediction model that combines with multidisciplinary analysis for clinical evaluation of malignancy risk of solid breast nodules

Bin Dong[1],*, Qiaohong Hu[2],*, Hongfeng He[2] and Ying Liu[2] ⓘ

Abstract

Objective: Few studies have systematically developed predictive models for clinical evaluation of the malignancy risk of solid breast nodules. We performed a retrospective review of female patients who underwent breast surgery or puncture, aiming to establish a predictive model for evaluating the clinical malignancy risk of solid breast nodules.

Method: Multivariable logistic regression was used to identify independent variables and establish a predictive model based on a model group (207 nodules). The regression model was further validated using a validation group (112 nodules).

Results: We identified six independent risk factors (X_3, boundary; X_4, margin; X_6, resistive index; X_7, S/L ratio; X_9, increase of maximum sectional area; and X_{14}, microcalcification) using multivariate analysis. The combined predictive formula for our model was: $Z = -5.937 + 1.435X_3 + 1.820X_4 + 1.760X_6 + 2.312X_7 + 3.018X_9 + 2.494X_{14}$. The accuracy, sensitivity, specificity, missed diagnosis rate, misdiagnosis rate, negative likelihood ratio, and positive likelihood ratio of the model were 88.39%, 90.00%, 87.80%, 10.00%, 12.20%, 7.38, and 0.11, respectively.

Conclusion: This predictive model is simple, practical, and effective for evaluation of the malignancy risk of solid breast nodules in clinical settings.

*These authors contributed equally to this work.

Corresponding author:
Ying Liu, Department of ultrasonography, Zhejiang Provincial People's Hospital & People's Hospital of Hangzhou Medical College, No. 158 Shangtang Road, Hangzhou, Zhejiang 310014, China.
Email: sag1002@126.com

[1]Zhejiang Chinese Medical University, Hangzhou, Zhejiang, China
[2]Department of ultrasonography, Zhejiang Provincial People's Hospital & People's Hospital of Hangzhou Medical College, Hangzhou, Zhejiang, China

Introduction

The incidence of breast nodules is high worldwide, but optimal strategies for clinical assessment and treatment remain controversial.[1] The consensus of many studies has been that 20% to 30% of breast nodules will ultimately develop into cancer.[2] Early diagnosis and intervention is crucial for improving the prognosis of patients with breast cancer. Therefore, differentiating malignant nodules from benign lesions is of critical importance.

Only 1% to 2% of detected nodules are determined to be cancerous. However, the discovery of breast nodules often causes patients to worry because clinical evaluation of malignancy without pathological assessment is uncertain, and performing biopsies on some nodules can be difficult.[3] A bulletin published by the American College of Obstetricians and Gynecologists on Diagnosis and Management of Benign Breast Disorders[4] suggests that biopsy should be performed for women aged >30 years with low-risk nodules (Breast Imaging Reporting and Database System [BI-RADS] score 1–3) if cancerous properties are suspected based on imaging examination. However, BI-RADS grading of some nodules can be ambiguous.

Ultrasound is the most widely used imaging examination in the diagnosis of breast diseases.[5] The rate of early identification has markedly improved[6] with the application of novel ultrasonic techniques including contrast-enhanced ultrasound[7,8] and ultrasound elastography.[9,10]

Irregular spiculate or foliar margins, S/L ratio > 1, hypoechoic mass, microcalcification, and arterial flow with resistive index (RI) > 0.7 are considered typical ultrasonic manifestations associated with malignant nodules.[11–13] Mammography is an effective and clinically recognised method for early detection of microcalcification.[14] Magnetic resonance imaging (MRI) can detect microvessels around early lesions. Mortality rates associated with breast cancer have been significantly reduced by early identification of malignant nodules using these imaging techniques.[15,16] However, each technique has limitations and may not be accurate when applied independently. Thus, a combination of these technologies may improve diagnostic accuracy.

Studies[17,18] have pointed out that age should be considered a risk factor for the occurrence of breast cancer because patients over 40 years old have higher incidence. Currently, cancer antigen 15-3 (CA153) produced by breast cancer cells is the most specific biomarker.[19,20] Carcinoembryonic antigen (CEA), another specific marker, has been implicated as a diagnostic and prognostic indicator in breast cancer for nearly 30 years.[19–21] Additionally, family history is also an important risk factor.[22,23] Thus, multidisciplinary analysis to evaluate malignancy risk of breast nodules can increase the accuracy of diagnosis.

In the present study, we established a logistic regression model based on multidisciplinary analysis of data from imaging, serological, and clinical diagnostic

techniques to predict the malignancy risk of breast nodules.

Methods

Patients

This was a retrospective study based on clinical data obtained from female patients aged 20 to 78 years admitted to Zhejiang Provincial People's Hospital with solid breast nodules from January 2016 to June 2019. Ethical approval for this study was obtained from the Institutional Review Board of Zhejiang Provincial People's Hospital. As a retrospective study of anonymised imaging and clinical data, the requirement for informed consent was waived.

The inclusion criteria were as follows: 1) solid breast nodules were detected via ultrasound examination in our department using a GE Logiq E9 instrument (GE, Boston, MA, USA); 2) clinical information (ultrasonic, serological, clinical and mammography data) was complete; 3) patients underwent breast surgery or puncture in our hospital; and 4) pathological results were available. The exclusion criteria were: 1) nodules with unclear ultrasonic images or incomplete patient information; and 2) nodules without pathological results.

Variable Acquisition

The variables in the model were grouped as shown in Table 1. Ultrasonic variables were grouped as follows: a) nodule size (maximum diameter); b) internal echo (hyperecho, isoecho, or hypoecho); c) boundary (well-defined or poorly-defined); d) margin (regular or irregular); e) colour Doppler flow imaging (without blood flow, dotted blood flow, or abundant blood flow); f) RI >0.7 or <0.7; g) S/L ratio >1.0 or <1.0; h) elastography score (1–5); and i)

Table 1. Variable name and assignment of values.

Variable	Variable name	Assignment
Malignant nodule	Y	Yes, $Y = 1$; no, $Y = 0$
Nodule size (maximum diameter), mm	X_1	Continuous variable
Internal echo	X_2	Hyperecho/isoecho, $X_2 = 0$; hypoecho, $X_2 = 1$
Boundary	X_3	Well-defined, $X_3 = 0$; ill-defined, $X_3 = 1$
Margin	X_4	Regular, $X_4 = 0$; irregular, $X_4 = 1$
CDFI	X_5	Without flow/ dotted flow, $X_5 = 0$; abundant blood flow, $X_5 = 1$
RI	X_6	<0.7, $X_6 = 0$; >0.7, $X_6 = 1$
S/L ratio	X_7	<1, $X_7 = 0$; >1, $X_7 = 1$
Elastography score	X_8	Score 1–2, $X_8 = 0$; score 3–5, $X_8 = 1$
Increase in maximum sectional area	X_9	Yes, $X_9 = 1$; no, $X_9 = 0$
CA153, μg/L	X_{10}	Continuous variable
CEA, μg/L	X_{11}	Continuous variable
Age > 40 years	X_{12}	No, $X_{12} = 0$; yes, $X_{12} = 1$
Family history	X_{13}	No, $X_{13} = 0$; yes, $X_{13} = 1$
Microcalcification	X_{14}	No, $X_{14} = 0$; yes, $X_{14} = 1$

CA153, cancer antigen 15-3; CDFI, colour Doppler flow imaging; CEA, carcinoembryonic antigen; RI, resistive index.
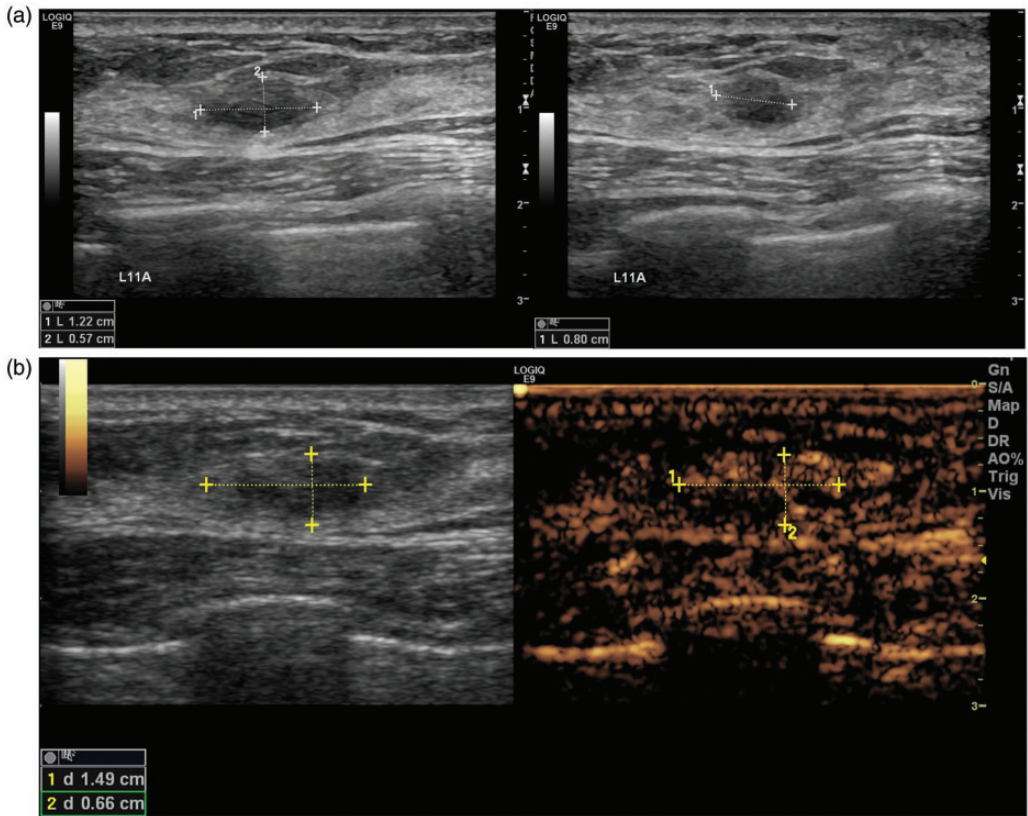
Figure 1. Contrast-enhanced ultrasonography of a solid breast nodule. (a) Using two-dimensional ultrasonography, the size of the nodule was 12.2 mm by 5.7 mm. (b) Using contrast-enhanced ultrasonography, the size of the nodule was 14.9 mm by 6.6 mm, and thus the maximum sectional area increased.

increase or no increase in the maximum sectional area of the nodule using contrast-enhanced ultrasound (Figure 1). Serological variables included levels of the tumour markers CA153 and CEA (μg/L). Clinical variables included age (>40 years or <40 years) and family history of breast cancer (present or absent). Mammography variables included microcalcification features based on molybdenum target mammography (present or absent) (Figure 2).

Variable Assignment

Table 1 shows the method of variable assignment. Pathological diagnosis (benign or malignant) of solid breast nodules was

used as the dependent variable, and the above 13 multidisciplinary variables were used as independent variables. All variables except nodule size, RI, L/R ratio, CA153, and CEA were categorical variables.

To reduce bias, the X_2, X_3, X_4, X_5 and X_8 ultrasound variables were assessed independently by two physicians with more than 5 years of experience in ultrasound diagnosis of breast diseases. Kappa values were calculated and variables with poor consistency were eliminated.

Data Processing and Statistical Analysis

To estimate malignancy risk, 207 nodules were randomly selected from the 319
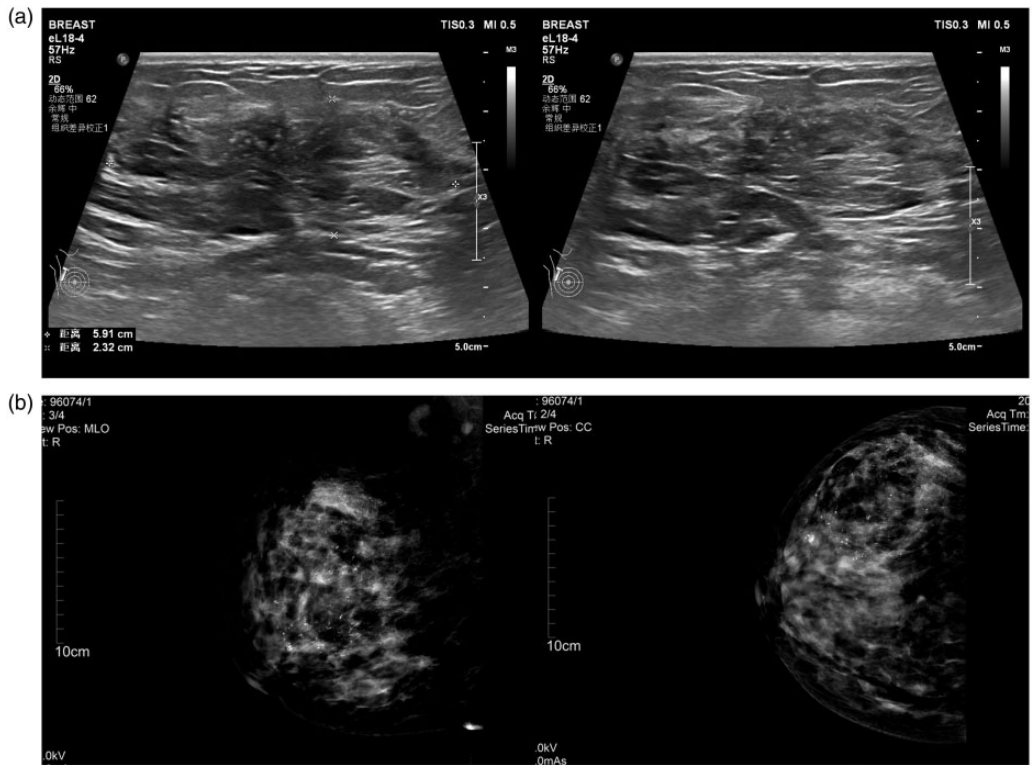
Figure 2. Microcalcification of a solid breast nodule. (a) Microcalcifications shown by ultrasonography. (b) Microcalcifications shown by mammography.

nodules and were defined as the model group. The remaining 112 nodules were defined as the validation group. The model was evaluated based on various performance measures (accuracy, sensitivity, specificity, Jorden index, missed diagnosis rate, negative likelihood ratio, and positive likelihood ratio).

To reduce bias, two ultrasound physicians with more than 5 years of experience performing thyroid ultrasounds measured ultrasonic variables. Kappa analysis was performed on subjective variables (X_2, X_3, X_4, X_5, and X_8). Variables with poor consistency were eliminated. Variables in the benign and malignant groups were first investigated by univariate analysis. Variables showing no significant difference were excluded, and logistic regression analysis was performed using the remaining variables.

To establish the predictive model, multivariable logistic regression was performed on the 207 nodules in the model group. The odds ratio (OR) of each variable was calculated using the formula $Z = \mathrm{Logit}(P) = \ln[P/(1-P)] = \beta_0 + \beta_1 X_1 + \beta_2 X_2 + \cdots + \beta_{14} X_{14}$, where $OR = e^{\beta}$; β is the regression coefficient. The predictive probability of malignancy was determined using P-values (inclusion criteria: $P < 0.05$; exclusion criteria: $P > 0.1$). Variables with no ability to differentiate benign from malignant nodules were eliminated.

To validate the predictive model, values of regression parameters were estimated using likelihood ratio tests. The goodness of fit of the entire model was evaluated

Table 2. Consistency analysis of subjective variables.

Variable	X_2	X_3	X_4	X_5	X_8
Kappa value*	0.787	0.749	0.836	0.768	0.756
P	<0.001	<0.001	<0.001	<0.001	<0.001

*Kappa values >0.75 were considered to indicate substantial consistency, values of 0.40–0.75 indicated moderate consistency, and values <0.40 indicated poor consistency. For the identity of variables and variable name assignment, refer to Table 1.

using the Hosmer–Lemeshow (H-L) test. Predictions of malignant and benign solid breast nodules were made using thresholds of $P \geq 0.05$ and $P < 0.05$, respectively. This criterion was used as the standard in subsequent large-sample validation experiments. Prevalence rates in the validation group were calculated and validated by pathological assessment. The diagnostic efficiency of the model was verified against the validation group using the performance indices mentioned above.

To further assess the diagnostic value of the model, diagnostic efficiency of each variable was evaluated via receiver operating characteristics curve (ROC) analysis. The model was compared with the gold standard, pathological assessment.

Results

Patients

A total of 319 female patients aged 20 to 78 years (mean ± standard deviation [SD]: 41.46±12.967 years) admitted to Zhejiang Provincial People's Hospital with solid breast nodules from January 2016 to June 2019 were enrolled in the study. Among 319 nodules with lengths ranging between 3.5 and 84.0 mm (mean ± SD: 19.50 ± 14.77 mm), 232 and 87 nodules were determined as benign and malignant, respectively, based on further pathological examinations.

Kappa Analysis

Table 2 shows the Kappa values for the X_2, X_3, X_4, X_5, and X_8 ultrasound variables. All were ≥0.75, indicating high consistency.

Univariate Analysis (Independent Sample T-Test and Chi-Square Test)

Table 3 shows the univariate statistical analysis of all 13 variables. The X_1, X_2 and X_8 variables did not reach statistical significance and were removed. We analysed the remaining 10 variables using multivariable logistic regression to further identify variables of clinical significance.

Establishment of Predictive Model

Table 4 shows the independent variables (including X_3, X_4, X_6, X_7, X_9, and X_{14}) that were ultimately included in the model. The combined predictive formula of the model was as follows: $Z = -5.937 + 1.435X_3 + 1.820X_4 + 1.760X_6 + 2.312X_7 + 3.018X_9 + 2.494X_{14}$; $P = e^z/1 + e^z$, where P denotes the morbidity rate and e represents the natural logarithm (2.72).

Validation of Predictive Model

The H-L test yielded a P-value of 0.574, indicating a good fitting effect with a high coefficient of determination ($R^2 = 0.801$). This suggested that the model had high predictive accuracy. Malignant and benign nodules were identified using thresholds of $P \geq 0.5$ and $P < 0.5$ values, respectively. In

Table 3. Univariate statistical analysis.

	Malignant nodules (57)	Benign nodules (150)	t/χ^2	P
X_1, mm	22.53 ± 13.89	18.35 ± 14.88	-1.836	0.068
X_2, n (%)				
0	9 (15.79)	30 (20.00)	0.479	0.489
1	48 (84.21)	120 (80.00)		
X_3, n (%)				
0	18 (31.58)	132 (88.00)	65.895	<0.001
1	39 (68.42)	18 (12.00)		
X_4, n (%)				
0	18 (31.58)	105 (70.00)	25.287	<0.001
1	39 (68.42)	45 (30.00)		
X_5, n (%)				
0	21 (36.84)	96 (64.00)	12.397	<0.001
1	36 (63.16)	54 (36.00)		
X_6, n (%)				
0	6 (10.53)	114 (76.00)	72.672	<0.001
1	51 (89.47)	36 (24.00)		
X_7, n (%)				
0	12 (21.05)	129 (86.00)	80.223	<0.001
1	45 (78.95)	21 (14.00)		
X_8, n (%)				
0	21 (36.84)	78 (52.00)	3.803	0.051
1	36 (63.16)	72 (48.00)		
X_9, n (%)				
0	18 (12.00)	147 (98.00)	112.672	<0.001
1	39 (88.00)	3 (2.00)		
X_{10}, μg/L	9.132 ± 12.93	4.250 ± 6.04	-1.582	0.129
X_{11}, μg/L	4.58 ± 5.49	2.82 ± 3.50	-1.579	0.119
X_{12}, n (%)				
0	12 (21.05)	66 (44.00)	9.262	0.002
1	45 (78.95)	84 (56.00)		
X_{13}, n (%)				
0	45 (78.95)	141 (94.00)	10.267	<0.001
1	12 (21.05)	9 (6.00)		
X_{14}, n (%)				
0	12 (21.05)	135 (90.00)	95.390	<0.001
1	45 (78.95)	15 (10.00)		

Data are presented as n (%) or mean ± standard deviation. *P*-values are derived from t-tests or chi-square tests. For the identity of variables and variable name assignment, refer to Table 1.

the validation group, 30 malignant and 82 benign nodules were identified by pathological assessment. In addition, 37 malignant and 75 benign nodules were subjected to prediction using the model. The model correctly predicted 27 malignant nodules while missing three, and correctly diagnosed 72 benign nodules while misdiagnosing 10. The accuracy, sensitivity, missed diagnosis rate, specificity, misdiagnosis rate, positive likelihood ratio, and negative likelihood ratio of the model were 88.39%, 90.00%, 10.00%, 87.80%, 12.20%, 7.38, and 0.11, respectively.

Table 4. Results of logistic regression.

Variable	B*	SE	Wald	df	P	Exp(B)§
X_3	1.435	0.658	4.753	1	0.029	4.198
X_4	1.820	0.702	6.712	1	0.010	6.171
X_6	1.760	0.606	8.429	1	0.004	5.812
X_7	2.312	0.569	16.524	1	<0.001	10.091
X_9	3.018	0.733	16.946	1	<0.001	20.443
X_{14}	2.494	0.683	13.323	1	<0.001	12.112
Constant	−5.937	0.738	64.720	1	<0.001	0.003

*B is the coefficient
§Exp(B) is the odds ratio of the corresponding variable.
df, degrees of freedom; SE, standard error. For the identity of variables and variable name assignment, refer to Table 1.
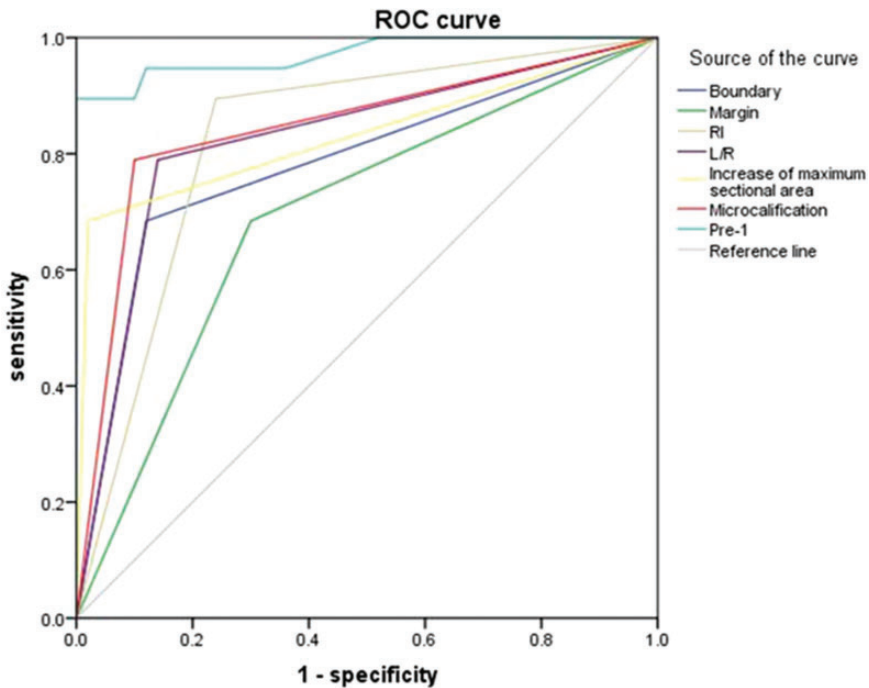

Figure 3. Receiver operator curve analysis of the whole predictive model the selected model variables. Pre-1 represents the whole model. The areas under the curve for X_3, X_4, X_6, X_7, X_9, X_{14}, and the whole model were 0.782, 0.692, 0.827, 0.825, 0.832, 0.845, and 0.971, respectively. For the identity of variables and variable name assignment, refer to Table 1.

Evaluation of Diagnostic Efficiency

The results of ROC curve analysis of the model and each selected variable are summarised in Figure 3. The area under the curve for the X_3, X_4, X_5, X_6, X_7, and X_{13} variables and for the whole model were 0.782, 0.692, 0.636, 0.827, 0.825, 0.845, and 0.954, respectively. These datas indicated that the diagnostic accuracy of the

overall model was higher than that of each single variable.

Discussion

The morbidity and mortality of breast cancer has increased worldwide in recent years.[24] Breast cancer is one of the most frequent malignant tumours in women. Therefore, early detection and diagnosis is crucial for effective treatment and satisfactory prognosis. Previous studies investigating the early identification and diagnosis of breast cancer[25–27] did not assess multiple variables. The clinical significance of comprehensive interdisciplinary and multivariate diagnostic criteria for differential diagnosis of benign and malignant breast nodules has not been widely investigated.

In the present study, differences among multiple variables were analysed using logistic regression. According to previous studies,[19–21] ultrasound, mammography, CA153 and CEA, age, and family history are factors relevant for differential diagnosis. The objectivity and accuracy of prediction improved when these parameters were included. During the establishment of the logistic regression model, variables without predictive value were excluded to improve stability of the model. Screening of successive regression models identified the following significant predictors of malignancy: unclear boundary, irregular shape, RI >0.7, L/R >1, increased maximum section area of nodules after contrast-enhanced ultrasound (relative to two-dimensional ultrasound), family history, and microcalcification identified via mammography. All regression coefficients were >0 and P values were <0.05. These data above demonstrated the critical value of previously identified indicators for evaluating the malignancy risk of breast nodules. A nodule with more positive indicators would be more likely to be malignant.

ORs for all variables in the model were compared and the importance of previously identified indicators for risk assessment was assessed. Variable X_{14}, microcalcification, had the highest OR, representing higher risk assessment value compared with other variables. As shown by goodness-of-fit tests, our predictive model exhibited high accuracy and a good fitting effect. These data demonstrate that comprehensive assessment of multidisciplinary variables is more effective for assessment of malignancy risk in breast nodules compared with analysis of single variables.

At present, needle biopsy is the preferred method for differential diagnosis of breast nodules before surgery.[28,29] However, invasive biopsy may cause complications such as bleeding, infection, and nerve damage, particularly in elderly or sick patients.

Our regression model could identify predictive indicators associated with malignancy risk of solid breast nodules, thereby improving the accuracy of differential diagnosis. The model may assist physicians in making more accurate diagnoses, avoid unnecessary needle biopsy, assist clinicians in formulating better treatment decisions, and guide postoperative follow-up.

Our study had several limitations. First, several eliminated variables may still be closely related to the occurrence and development of breast cancer. Second, to integrate patient information and to maintain a large sample size, we had to remove microvessels around early lesions in MRI scans, serum ferritin, procalcitonin, and other features potentially associated with malignancy. Last, as a retrospective analysis, the reliability of our conclusions depended on the sample size. In future work, we plan to further enlarge the sample size to verify the clinical applicability of this model.

Conclusion

A predictive model for evaluation of the malignancy risk of solid breast nodules was established. Based on multivariable logistic regression analysis, the model included multiple indicators of malignant nodules. This model may provide social and economic benefits via improved accuracy of diagnosis.

ORCID iD

Ying Liu 🆔 https://orcid.org/0000-0002-5675-0623

References

1. Wang YN and Wang Q. Evaluation, diagnosis and treatment of breast nodules. *Chinese J Breast Dis (Electron Ed)* 2016; 10: 321–325.
2. Zhao HJ, Wang J, Wang QL, et al. Retrospective analysis of regular follow-up results of mammary gland hyperplasia patients with small diameter mammary nodules. *Chin J Obstet Gynecol Pediatr (Electron Ed)* 2016; 12: 608–612.
3. Zhang Y, Zhao CK, Li XL, et al. Virtual touch tissue imaging and quantification: Value in malignancy prediction for complex cystic and solid breast lesions. *Sci Rep* 2017; 7: 7807.
4. American College of Obstetricians and Gynecologists' Committee on Practice bulletins. Gynecology practice bulletin no. 164: Diagnosis and management of benign breast disorders. *Obstet Gynecol* 2016; 127: e141–e156.
5. Tang L, Xu HX, Bo XW, et al. A novel two-dimensional quantitative shear wave elastography for differentiating malignant from benign breast lesions. *Int J Clin Exp Med* 2015; 8: 10920–10928.
6. Zhou HM, Ran HT and Cheng J. Status of new ultrasonic technology combined with breast imaging-reporting and data system for ultrasound in evaluating breast lesions. *Chinese J Interv Imaging Ther* 2018; 15: 188–191.
7. Gilbert FJ and Pinker-Domenig K. Diagnosis and staging of breast cancer: When and how to use mammography, tomosynthesis, ultrasound, contrast-enhanced mammography, and magnetic resonance imaging. In: Hodler J, Kubik-Huch RA, von Schulthess (eds) *Diseases of the chest, breast, heart and vessels 2019–2022: Diagnostic and interventional imaging.* Cham: Springer, 2019, pp. 155–166.
8. Kim Y, Kim SH, Song BJ, et al. Early prediction of response to neoadjuvant chemotherapy using dynamic contrast-enhanced MRI and ultrasound in breast cancer. *Korean J Radiol* 2018; 19: 682–691.
9. Sigrist R, Joy L and El KA, et al. Ultrasound elastography: Review of techniques and clinical applications. *Theranostics* 2017; 7: 1303–1329.
10. Kapetas P, Clauser P, Woitek R, et al. Quantitative multiparametric breast ultrasound: Application of contrast-enhanced ultrasound and elastography leads to an improved differentiation of benign and malignant lesions. *Invest Radiol* 2019; 54: 257–264.
11. He Y, Wang XY, Ling B, et al. Characteristic of ultrasonography and contrast-enhanced ultrasound for the breast ductal carcinoma *in situ* correlation with pathology. *Chinese J Ultrasound Med* 2015; 31: 494–497.
12. Diao XH, Chen Y, Zhan J, et al. The application of multi-mode ultrasound blood technology in the perforating vessels of the breast lesions. *Chinese J Ultrasound Med* 2016; 32: 752–754.

13. Vaughan CL, Douglas TS, Said-Hartley Q, et al. Testing a dual modality system that combines full-field digital mammography and automated breast ultrasound. *Clin Imaging* 2016; 40: 498–505.

14. Fiorica JV. Breast cancer screening, mammography, and other modalities. *Clin Obstet Gynecol* 2016; 59: 688–709.

15. Greenwood HI, Freimanis RI, Carpentier BM, et al. Clinical breast magnetic resonance imaging: Technique, indications, and future applications. *Semin Ultrasound CT MR* 2018; 39: 45–59.

16. Ko ES and Morris EA. Abbreviated magnetic resonance imaging for breast cancer screening: Concept, early results, and considerations. *Korean J Radiol* 2019; 20: 533–541.

17. Coughlin SS. Epidemiology of breast cancer in women. *Adv Exp Med Biol* 2019; 1152: 9–29.

18. Radecka B and Zhang M. Breast cancer in young women. *Ginekologia Polska* 2016; 87: 659–663.

19. Li X, Dai D, Chen B, et al. Clinicopathological and prognostic significance of cancer antigen 15-3 and carcinoembryonic antigen in breast cancer: A meta-analysis including 12,993 patients. *Dis Markers* 2018; 2018: 3810–3814.

20. Yang ZA. The detective value of CEA, CA125 and CA153 in mammary cancer. *J Hunan Normal Univ (Med Sci)* 2016; 13: 83–85.

21. Wang JM and Zhu LR. Changes of serum carbohydrate antigen 15-3, carcinoembryonic antigen, ferritin and calcitonin in patients with breast cancer and their clinical significance. *China J Health Lab Tec* 2018; 28: 1605–1610.

22. Brewer HR, Jones ME, Schoemaker MJ, et al. Family history and risk of breast cancer: An analysis accounting for family structure. *Breast Cancer Res Treat* 2017; 165: 193–200.

23. Seven M, Bağcivan G, Akyuz A, et al. Women with family history of breast cancer: How much are they aware of their risk? *J Cancer Educ* 2018; 33: 915–921.

24. Siegel RL, Miller KD and Jemal A. Cancer statistics, 2020. *CA Cancer J Clin* 2020; 70: 7–30.

25. Milosevic M, Jankovic D, Milenkovic A, et al. Early diagnosis and detection of breast cancer. *Technol Health Care* 2018; 26: 729–759.

26. Winters S, Martin C, Murphy D, et al. Breast cancer epidemiology, prevention, and screening. *Prog Mol Biol Transl Sci* 2017; 151: 1–32.

27. Ding MX, Bai YH, Tang FZ, et al. Value of contrast-enhanced ultrasound combined with BI-RADS in the diagnosis of suspected breast cancer. *Pract J Cancer* 2018; 22: 1184–1186.

28. Calhoun KE and Anderson BO. Needle biopsy for breast cancer diagnosis: A quality metric for breast surgical practice. *J Clin Oncol* 2014; 32: 2191–2192.

29. Suh CH, Baek JH, Lee JH, et al. The role of core-needle biopsy in the diagnosis of thyroid malignancy in 4580 patients with 4746 thyroid nodules: A systematic review and meta-analysis. *Endocrine* 2016; 54: 315–328.